Effect of alteration on the geochemistry and mechanical properties of granite from Pingjiang, Hunan Province, China

Published in:
Environmental Earth Sciences

Publication Status:
Published (in print/issue): 20/01/2022

DOI:
https://doi.org/10.1007/s12665-022-10197-z

Document Version
Author Accepted version

Effect of alteration on the geochemistry and mechanical properties of granite from Pingjiang, Hunan Province, China

Minghao Ren[a*], Wei Wang[a], Zhiquan Huang[b*], Shanggao Li[c], Qi Wu[a], Huaichang Yu[a], Guangxiang Yuan[a], Paul Sargent[d]

[a] College of Geosciences and Engineering, North China University of Water Resources and Electric Power, Zhengzhou, 450046, China

[b] Luoyang Institute of Science and Technology, Luoyang 471023, China

[c] Zhongnan Engineering Corporation Limited, Changsha, 410014, China

[d] School of Computing, Engineering and Digital Technologies, Teesside University, Middlesbrough, Tees Valley, TS1 3BA, UK.

[*] Corresponding author:

Dr. Minghao Ren

E-mail: renmh@ncwu.edu.cn

Prof. Zhiquan Huang

E-mail: huangzhiquan@ncwu.edu.cn

Funding information:

This study is financially supported by grants from a National Key R&D Program of China (Grant No. 2019YFC1509704), the Natural Science Foundation of China (Grant No. 41803033, 41903034), Central Plains Science and Technology Innovation Leader Project (Grant No. 214200510030) and the

Research Foundation of North China University of Water Resources and Electric Power (No. 20171003).

Abstract: The effect of alteration on the geochemistry and mechanical properties of granite from Pingjiang, Hunan Province, China was investigated. Six weathered and fourteen hydrothermally altered samples in three adits were collected for mechanical strength tests, mineralogical and geochemical analysis. The types of alteration observed within the samples were chloritization and argillization~~, which weakened the granite~~. ~~Conversely,~~ Samples taken from a silicified fracture zone were enriched in ~~strengthened by the enrichment of~~ quartz. Weathering was observed to significantly weaken the granite whereas the effects of hydrothermal alteration on strength were more complex. The porosity increased with the enrichment of the altered minerals, indicating that the formation of altered minerals degrades the strength of physical bonds between minerals within the granite. ~~With increasing loss-on-ignition, the mechanical strength properties of the granite decline rapidly before reaching residual values. This implies that the mechanical strength decreases rapidly even at low degrees of alteration.~~ The granite Na_2O, CaO, K_2O, MgO and SiO_2 contents decreased while Fe_2O_{3T} increased due to weathering. Variations of major elements within the hydrothermally altered granite were distinguished from those observed in weathered samples – notably Mg was removed ~~from granite~~ whilst Si and Fe were generally stable during the hydrothermal alteration. Whereas the quartz-enriched samples gained Si ~~and loss~~ with slight depletions in Mg and Fe ~~slightly~~. Trace ~~elements~~ and rare earth elements were both removed in hydrothermal alteration. The variable behavior of major element was quantified by the mobility index~~. The variable mobility of the major elements~~ which indicated that the different geochemical changes were attributed to ~~in~~ chloritization and argillization. Furthermore, the mobility index of Mg ~~could be~~ was used to identify the dominated alteration in granite and evaluate the effects of chloritization and argillization. Generally, ~~the~~ chloritization was found to be more dominant than argillization in ~~could~~ weakening the granite ~~more effectively than argillization~~.

Keywords: Weathering, Hydrothermal alteration, Geochemistry, Mechanical strength properties, Granite

1. Introduction

The mineralogical, geochemical, and mechanical properties of rocks can be significantly changed by alteration (del Potro and Hürlimann, 2009; Huang et al., 2011; Julia et al., 2014; Moon and Jayawardane, 2004; Pola et al., 2012, 2014; Wang et al., 2015; Wyering et al., 2014). Almost all alteration occurs in two ways: (1) rocks interacting with water and other agents of atmosphere, which is called weathering (Fritz and Mohr, 1984; Moon and Jayawardane, 2004; Wang et al., 2013); and (2) hydrothermal fluids coming into contact with rocks causing chemical reactions. The latter process is referred to as hydrothermal alteration (Browne, 1978; Wyering et al., 2014).

The influence of weathering on the mechanical properties of rocks has been well studied (Arikan et al., 2007; Ceryan et al., 2008; Julia et al., 2014; Pola et al., 2012, 2014, Wyering et al., 2014). ~~From previous studies,~~ Weathering processes generally cause a reduction in the mechanical strength and durability properties of rocks – thereby defining a negative correlation with weathering degree (Arikan et al., 2007; Pola et al., 2012, 2014). According to Julia et al. (2014) and Wyering et al. (2014), the relationships between some mechanical parameters of rock (e.g. uniaxial compressive strength, compressional wave velocity, Young's modulus) and degree of weathering ~~degree~~ could be defined by exponential functions. The mineralogical and chemical changes are also recognized during weathering, whereby the presence of alumina-silicate minerals such as feldspars convert into clay minerals which further reduces ~~the~~ rock strength ~~of rocks significantly~~ (Arikan et al., 2007; Coggan et al., 2013; Wyering et al., 2014; Columbu et al., 2019, 2020). While, the previous studies were mainly focused on the weathered volcanic rocks ~~instead of~~ rather than intrusive igneous rocks, such as granite (Chigira et al., 2002; Duzgoren-Aydin et al., 2002; Sumner and Nel, 2002; Moon and Jayawardane, 2004; Yıldız et al., 2010; Wang et al., 2015; Columbu et al., 2019, 2020). Typically, hydrothermal alteration occurs at higher temperatures and pressures compared with weathering (Browne, 1978; Fritz and Mohr, 1984). Therefore, the effects of weathering and hydrothermal alteration on rocks strength will ~~should~~ be significantly different. Given the generally high-quality mechanical strength properties of granite, hydroelectric dams are often situated on such rocks, including the Three Gorges Dam in China (Chen, 1999). The strength of the altered granite is directly related to dam stability. Due to the affinities between altered granite and the presence of metallic ores, the geochemical effects of alteration on the granite have been well studied (Baker, 1985; Farmer and DePalol, 1987; Meller et al., 2014; Xu et al., 2021). However, the mechanical strength of such hydrothermally altered granites has received little attention (Lan et al., 2003; Chen et al., 2018; Qin et al., 2019).

In this study, a Mesozoic altered granite intrusion in Hunan Province, China has been investigated. The site location is to be developed as a pumped storage hydroelectric station, which will be fed by dammed upper and lower reservoirs. Six weathered and fourteen hydrothermally altered samples were collected from three adits, which were marked as PD2, PD3, and PD4. Mechanical strength tests, major and trace element analyses were undertaken to: (1) investigate the effects of alteration on the mechanical strength properties of the granite; and (2) identify the geochemical changes during weathering and hydrothermal alteration and examine the differences between these two processes.

2. Geological background

The study area is located in the southern Yangtze Block where the regional structure is controlled by the deep Xinning–Miluo and Changsha–Pingjiang faults (Fig. 1). From north to south, this area is divided into four regions by these two faults, namely (1) Dongting rift basin, (2) Mufu Mountain–Ziyun Mountain uplift, (3) Pingjiang–Changsha rift basin, and (4) Lianyun Mountain–Hengyang uplift (Fig. 1). The basement strata comprise the Lengjiaxi (Mesoproterozoic) and Banxi (Neoproterozoic) Group. Due to tectonism, the granite was widely intruded in this area from the Mesoproterozoic to Mesozoic, particularly during the late Mesozoic.

Granite samples were collected from Fushou Mountain, which is located in the northern part of the Pingjiang–Changsha rift basin (Fig. 2). This granite was intruded into the Lengjiaxi Group at ca. 165 Ma (Xu et al., 2009; Zhang, 1991). Field investigations have shown that the structure of this area is controlled mainly by seven faults (Fig. 2) and joints developed in the intrusion. Quartz veins and pegmatite dykes are distributed around the faults.

3. Sampling and analytical methods

The samples in this study were collected according to the specifications for rock testing in water conservancy and hydroelectric engineering of the People's Republic of China (DL/T 5368-2007). The weathered samples (WA) were collected at the entrances of the adits, whereas hydrothermally altered samples (HA) were collected along the adits. Five samples were collected at the end of the PD2, where there is a silicified fracture zone (SZ) (Fig. 2). The volumes of the collected samples were representative and adequate for analytical testing.

The mechanical strength tests were carried out first, whereby small sub-samples were retained for the determining the bulk density, particle density and mineralogy. The powered samples were prepared by the agate mortar for geochemical analysis.

3.1 Mechanical strength tests

Ultrasonic P-wave velocities (V_p) were measured on all intact samples pioro to strength testing. Size-corrected point load strength index ($I_{s(50)}$) testing was undertaken on irregularly shaped specimens, based on previously published methodologies (Kahraman et al., 2005; Moon and Jayawardane, 2004; Yang, 2007). The rock strength test was carried out in situ using the rebound method with a hammer, whereby strength values were represented by the rebound value (R) (Ma, 2014). The dry bulk density and particle density of samples were determined in the laboratory following the procedures presented in previous studies (Lv et al., 2012; Wang et al., 2013; Miao, 2017).

3.2 Mineralogical analysis

Thin sections of the granite samples were cut and subjected to observational analysis under a binocular petrographical microscope. Mineral compositions of the samples were determined with X-ray diffraction (XRD) at the Key Laboratory of Mineralogy and Metallogeny in the Guangzhou Institute of Geochemistry, Chinese Academy of Sciences, Guangzhou, China. A Bruker

D8 Advance diffractometer with Ni-filtered CuKα radiation was employed, consistent with the analytical conditions and procedure used by Ma et al. (2016).

3.3 Whole-rock major and trace elements

Major and trace element concentrations were analyzed at the State Key Laboratory of Geochemistry in the Guangzhou Institute of Geochemistry, Chinese Academy of Sciences, Guangzhou, China. A Rigaku ZSX100e X-ray fluorescence (XRF) spectrometer was used for major element determination, following the analytical procedures of Li et al. (2006). The analytical precision was generally better than ±2%. Trace elements were determined with a Thermo X Series II inductively coupled plasma–mass spectrometer (ICP–MS) following the procedures of Li et al. (2006),whereby the analytical precision was ±5%.

4. Results

4.1 Mechanical strength

The physical properties ~~parameters~~ of the granite are summarised in Table 1. The weathered (WA) granite yielded lower dry bulk densities (2.19 – 2.32 g/cm^3) compared with the fresh (F) and hydrothermally altered (HA) samples (2.65 g/cm^3 and 2.41 – 2.58 g/cm^3, respectively). The particle density values ~~are in the~~ ranged ~~of~~ between 2.58 – 2.67 g/cm^3. Total porosity was calculated from knowledge of dry bulk density and particle density using the equation of Brown (1981). The mechanical test data are listed in Table 2. The fresh sample yielded 4.33 km/s for V_p, 4,991 kPa for $I_{s(50)}$ and 30 for rebound value. The WA samples ~~showed~~ exhibited the lowest mechanical strength. The mechanical strength for most HA samples were lower than fresh sample except for one sample, namely XP4-200. Compared with the fresh samples, SZ samples in the silicified fracture zone possessed higher $I_{s(50)}$ (e.g. PD 2-2) ~~or~~ and V_p values (e.g. PD2-6).

4.2 Mineralogy analysis

The mineralogy of the granite consists of quartz (20% – 52%), orthoclase (20% – 45%), plagioclase (20% – 35%), and biotite (2% – 8%) (Fig. 3a), thereby classifying the granite intrusion as a 'monzogranite'. A cataclastic texture was recognized in some samples (Fig. 3b). Due to weathering and hydrothermal alteration, biotite and feldspar minerals have been partially altered to chlorite and clay minerals (including kaolinite, smectite, and illite), respectively (Fig. 3a–b). The WA samples were intensely to completely weathered. The results of XRD showed that the composition of the weathered samples was up to 70% clay minerals (e.g. XP4-2). In the fault fracture zone of PD2, the granite has been brecciated with an abundance of quartz veins (Fig. 3c). The SZ samples in this zone possessed high quartz contents (Fig. 3d) of up to 75% (PD2-4) according to the XRD analysis, as presented in Table 1.

4.3 Whole-rock major and trace elements

The major and trace element data are summarised in Table 2. Compared with the hydrothermally altered samples, weathered samples are characterised by higher concentrations of MgO (0.60–2.55 wt.%) and total Fe_2O_3 (Fe_2O_{3T}) (2.13–9.90 wt.%), with lower Na_2O (0.32–3.81 wt.%), K_2O (1.57–3.22 wt.%), and CaO (0.67–2.97 wt.%) concentrations. Due to the enrichment of quartz, the samples from the silicification zone are associated with high SiO_2 concentrations. The loss-on-ignition (LOI) values, which is an important parameter used to define the alteration degree of magmatic rocks, varied from 2.35 to 8.14 wt.% and 0.53 to 1.58 wt.% for weathered and hydrothermally altered samples, respectively. Generally, the fresh sample have the highest concentrations of trace elements. SZ samples have the variable contents of trace elements compared with HA samples (Table 1).

5. **Discussion**

5.1 Effects of alteration on mechanical strength properties

Previous studies have demonstrated ~~shown~~ that weathering significantly reduces the mechanical strength of rocks, especially for the highly and completely weathered samples (Julia et al., 2014; Moon and Jayawardane, 2004). The WA samples in this study were considered to be highly weathered, yielding the lowest recorded mechanical strength and dry bulk density values. According to the mineralogy analysis, the altered mineral content of the WA samples, including chlorite and clay minerals, were higher than that of the HA and fresh samples. The porosity and the altered mineral contents show a positive correlation (Table 1), indicating that the formation of altered minerals weaken the physical bonds between minerals within the granite. Therefore, the reduction of the mechanical strength of the WA granite may be attributed to chloritization and argillization.

The mechanical parameters of HA samples were variable compared with the fresh samples~~. The HA sample in PD4 exhibited the highest mechanical strength, whereas the HA samples in PD2 were generally weaker than the fresh sample~~ , thereby highlighting the complex effects of hydrothermal alteration (Fig. 4). SZ samples in PD2 were noted to have similar or even higher $I_{s(50)}$ and rebound values compared with the fresh sample (Fig. 4). Chloritization and argillization also occurred in the HA and SZ samples, but to a lower degree compared with the WA samples. The higher mechanical parameters of the SZ samples indicate that they were less affected by chloritization and argillization compared with WA samples and most HA samples (Fig. 4). The SZ samples were subjected to the replacement reaction during the formation of quartz veins, ~~which resulted from~~ as a result of interactions with Si-rich hydrothermal fluids (Lv et al., 2011). Therefore, the SZ samples have higher quartz contents compared with the other samples (Table 1). Due to the high frictional resistance of quartz, ~~the~~ SZ samples were strengthened rather than weakened by the enrichment of quartz.

The LOI value was assumed to represent the water retained within a rock and its minerals, which is regulated by the degree of weathering (Moon and Jayawardane, 2004; Pola et al., 2012). Water can be incorporated into the structures of secondary minerals during the hydrothermal alteration (Hurwitz et al., 2002; Pola et al., 2012, 2014; Wyering et al., 2014; Julia et al., 2014). Therefore, the LOI value is also an indicator of the degree of hydrothermal alteration. The mechanical parameters of all samples declined rapidly when the LOI values range from 0 to 2 wt.%, beyond which they were relatively constant (Fig. 5). According to previous studies, the relationships between ~~the~~ mechanical strength and the degree of alteration could be defined by the exponential equations (Julia et al. 2014; Wyering et al. 2014). However, ~~this was not clearly~~ such expressions were not appropriate to ~~observed in~~ this study (Fig. 5). The unclear relationships between mechanical strength parameters and the degree of alteration may be attributed to two reasons: (1) the heterogeneity of the granite – meaning that samples have inconsistent initial strength before alteration, and (2) the complexity of the alteration effects. As mentioned above, the chloritization and argillization could weaken the granite while the enrichment of quartz could strengthen them.

In addition, the reported correlation coefficients for the relationship between mechanical strength and degree of alteration were in the range of 0.6-0.8 (Julia et al., 2014; Wyering et al., 2014). Instead of LOI, porosity was used as a parameter to quantify the degree of alteration within samples from previous studies (Julia et al., 2014; Wyering et al., 2014). In this study, the porosity of granite increased with the enrichment of the altered minerals (Table 1). Although the porosity has a strong influence over the mechanical strength of rocks, it can also be affected by various other factors including grain size, mineral composition and microstructure (Ulusay et al., 1994; Li and Aubertin, 2003; Palchik and Hatzor, 2004; Baud et al., 2014; Ündül, 2016). Therefore, porosity was partly ~~not fully~~ partially controlled by the alteration degree of rocks, which is especially pertinent for volcanic rocks, which are usually more porous due to their vesicular structure (Saar and Manga, 1999; Shea et al., 2010; Heap et al., 2014). The variable effects of hydrothermal alteration within HA samples indicates that hydrothermal alteration could affect not only porosity but also other controlling factors of mechanical strength of granite. A further study including more investigations on texture and porosity of hydrothermally altered granite is necessary to better understand the conditions that are responsible for the different effects of hydrothermal alteration.

5.2 Geochemical changes due to alteration

Generally, mineral alterations are accompanied by geochemical variations. Many studies have documented geochemical changes resulting from weathering of magmatic rocks, especially the volcanic and pyroclastic rocks (Aiuppa et al., 2000; Chigira et al., 2002; Columbu et al., 2019, 2020; Duzgoren-Aydin et al., 2002; Fritz and Mohr, 1984; Guan, 2001; Lan et al., 2003; Moon and Jayawardane, 2004; Sharma and Rajamani, 2000). From these previous studies, the alteration of volcanic and pyroclastic rocks is considered to be mainly due to the devitrification of their glassy matrices ~~within these rocks~~, resulting in the formation of new minerals (e.g. phyllosilicates). Furthermore, weathering increased the mineralogical and geochemical changes of rocks, favoring the formation of clay minerals (Columbu et al., 2019, 2020). Na, Ca, Si, K, and Mg are mobile, whereas Zr, Ti, and Al are immobile during weathering. Thus, Na_2O, CaO, SiO_2, K_2O, and MgO would be leached from rocks during weathering. FeO would be oxidized to Fe_2O_3 during weathering, thereby increasing the total Fe_2O_3 content and decreasing the FeO content (Aiuppa et al., 2000; Chigira et al., 2002; Guan, 2001; Moon and Jayawardane, 2004; Columbu et al., 2019, 2020;). Most trace element concentrations increase during early weathering stages but decrease as weathering progresses further. Such increases in concentration during the early stages are likely to be a reflection of the loss of major elements, whilst concentration reductions likely represent the mobilization of trace elements during argillization (Aiuppa et al., 2000; Moon and Jayawardane, 2004). Rb and Sr behave similarly to Ca during weathering due to their similar ionic radii properties (Moon and Jayawardane, 2004).

The results for weathered samples in this study are similar to those of previous studies. Na_2O, CaO, K_2O, and SiO_2 contents in the weathered samples showed negative correlations with LOI values (Fig. 6a–d), meaning that contents of these elements decreased during weathering. Fe_2O_{3T} concentrations increased significantly with increasing LOI ~~increased~~ (Fig. 6f). However, MgO concentrations were different than those described in some previous studies (Guan, 2001; Moon and Jayawardane, 2004). MgO contents in the weathered samples showed a positive correlation with LOI values, indicating that the samples gained MgO during weathering (Fig. 6e). A similar increase in MgO within weathered samples was reported by Chigira et al. (2002). The inconsistent behavior of MgO may be attributed to variations in alteration during the weathering (Aiuppa et al., 2000; Chigira et al., 2002; Guan, 2001; Moon and Jayawardane, 2004).

The geochemical changes of the granite during hydrothermal alteration were complex and mainly depend upon the types and conditions of alteration (Baker, 1985; Farmer and DePalol, 1987; Wang et al., 2013; Meller et al., 2014; Wyering et al., 2014; Xu et al., 2020). The loss of Ca, Na and Fe is reported when biotite and plagioclase are altered to muscovite and clay minerals (Xe et al., 2020). During albitization of granite, Na, Si and Mg are added, while K and Fe are lost (Baker, 1985). In this study, major elements of the hydrothermal altered samples showed no clear relationship with LOI and the variation trends are distinguished from weathering (Fig. 6). Na and K can be depleted but also enriched during the hydrothermal alteration (Fig. 6a, c). Ca was largely removed from granite (Fig. 6b). Si and Fe were generally stable during the hydrothermal alteration (Fig, 6d, f). The quartz-enriched samples yielded the addition of Si (Fig. 6d) and ~~slightly~~ small losses of Mg and Fe (Fig. 6e, f). The trace elements and rare earth elements (REE) in hydrothermally altered samples were depleted; in only one sample (PD2-2) were heavy REE introduced (Fig. 7a, b). ~~The depletion of~~ REE depletion during the chloritization and argillization was reported, whereas the enrichment of heavy REE were attributed to the affinities of heavy REE in chlorites (Alderton et al., 1980; Baker, 1985; Dawood et al., 2005; Xu et al., 2020). In addition, the trace elements and REE of the SZ samples varied in a wider range compared with the HA samples (Fig. 7a, b).

The mobility of major elements could be quantitively evaluated with the mobility index (MI), which was described by Guan et al. (2001). Based on fieldwork and petrological observations, samples from PD2 and PD3 were noted to have similar mineral compositions. Therefore, these samples were ideal for assessing element mobility due to weathering and hydrothermal alteration. The calculated activities of Al species in weathering and many hydrothermal systems are very low, and Al is conserved during the conversion of biotite to chlorite (Helgeson, 1970; Parry and Downey, 1982). Therefore, Al_2O_3 was taken to be immobile elements, and the unaltered sample PD2-7 was used as the baseline sample to assess alteration effects. The MI of major element was then calculated as follows:

$$MI = (R^i_a/R_a)/(R^i_p/R_p) \quad (1)$$

where R^i_a is the weight percentage of mobile element *i* in the altered sample, R_a is the weight percentage of immobile elements in the altered sample, R^i_p is the weight percentage of mobile element *i* in the unaltered sample, and R_p is the weight percentage of immobile elements in the unaltered sample.

The calculated MI for major elements normalized to Al_2O_3 are shown in Fig. 8. The enrichment of Mg and Fe distinguish weathered samples from hydrothermally altered sample. The Si is generally immobile but could be mobilized during the quartz-enrichment. As mentioned above, the alterations in weathered and hydrothermally altered granite were both chloritization and argillization. Therefore, the mobility of elements is supposed to be similar in weathered and hydrothermally altered granite. The variable mobility of the major elements indicates the different geochemical changes in chloritization and argillization.

5.3 Differences in element mobilities due to alteration

Argillization and chloritization occur under different thermal conditions and by distinct processes. Argilliaceous rocks are formed at low temperatures (50–150℃) (Julia et al., 2014). During the early stages of argillization, plagioclase reacts with K-rich acidic hydrothermal fluids, forming smectite/illite. As the reaction progresses, H^+ replaces K^+ in K-feldspar and smectite/illite, forming kaolinite. The major compositional change in the rock is the removal of Ca, Na, and some Mg. K tends to remain constant, or slightly increases and then decreases (Hemley and Jones, 1964). Thus, changes in K and the loss of Ca and Mg in the altered samples of this study are attributed mainly to argillization (Fig. 8). However, changes in Na content are not consistent with argillization, as the HA and SZ samples were observed to increase in ~~gained~~ Na content (Fig. 8). Thin-section observations revealed that orthoclase was partially altered to albite (Fig. 3a). During this process, K was replaced by Na, thereby increasing the Na concentration. Therefore, the formation of albite might be responsible for the increases in Na in the altered samples.

The temperatures of chlorite formation are 150–300°C (Huang, 2017). Previous studies have concluded that the alteration of biotite to chlorite in granite conserves Al, resulting in the loss of K and Ti, along with the gain of Mg and Mn (Parry and Downey, 1982). Therefore, the enrichment of Mg can be attributed to chloritization. Quartz-enrichment occurs due to reactions with high-temperature fluids (300–550℃) (Julia et al., 2014). This process significantly increases SiO_2 concentrations of samples in two ways: (1) SiO_2 derived from the hydrothermal fluids and (2) by decomposition of feldspar to clay minerals (e.g. argillization; Lv et al., 2011). In this study, the MI of SiO_2 in the non-silicified samples are all near unity (Fig. 7). As such, silicification associated with argillization was negligible. Therefore, the SiO_2 added to the silicified samples was derived from hydrothermal fluids. The variable trace elements and REE in the SZ samples also indicate that the chloritization and argillization may be motivated in this process (Fig. 7a, b).

As mentioned above, Mg is noted to be enriched by chloritization while depleted by argillization. Therefore, the MI of Mg could be used to identify the dominated alteration when these two types of alteration both occurred. The chloritization-dominated samples were expected to have a high MI of Mg (higher than 1) while the MI of Mg within the argillization-dominated samples should be lower than 1. Generally, the argillization-dominated samples have the higher mechanical strength parameters (e.g. average of $I_{s(50)}$ = 3,555 kPa) compared with the chloritization-dominated samples (e.g. average of $I_{s(50)}$ = 1,150 kPa). This may indicate that the chloritization could weaken the granite more effectively.

6. Conclusions

The effects of alteration on the mechanical properties of granite were investigated using mechanical tests and geochemical data. Due to the high grade of weathering, weathered monzogranites have a ~~much~~ low mechanical strength whereas the strengths measured for hydrothermally altered monzogranites were more variable. The porosity increased with the enrichment of the altered minerals, indicating that the formation of altered minerals weaken the physical bonds between minerals within the granite. Monzogranite was weakened by argillization and chloritization, ~~whereas it is~~ but strengthened by the enrichment of quartz. ~~With increasing loss-on-ignition, the mechanical strength properties of the granite declined rapidly before reaching residual~~

~~values. As such, mechanical strength decreases rapidly at low degrees of alteration.~~ A further study on hydrothermally altered granite is necessary to identify and better understand the conditions corresponding to the different effects of hydrothermal alteration on mechanical strength.

Granite Na_2O, CaO, K_2O, MgO and SiO_2 contents decreased while Fe_2O_{3T} increased due to weathering. Variations of major elements within the hydrothermally altered granite were distinguished from those within weathered samples. Ca was removed from granite significantly while Si and Fe were generally stable during the hydrothermal alteration. The quartz-enriched samples gained Si, whilst losing some ~~and loss~~ Mg and Fe contents ~~slightly~~. The trace ~~elements~~ and rare earth elements were both removed in hydrothermal alteration. The variable behavior of major element was quantified by the mobility index. The variable mobility of the major elements indicates the different geochemical changes in chloritization and argillization.

Argillization and chloritization occur under different thermal conditions and by distinct processes, leading to the different characteristics of the elements. Mg could be enriched by chloritization while depleted by argillization. This observation ~~could be~~ was used to identify the dominant type of alteration in granite and evaluate the effects of chloritization and argillization. Generally, the chloritization ~~could~~ was noted to weaken the granite more than argillization.

Acknowledgements

This study is financially supported by grants from a National Key R&D Program of China (Grant No. 2019YFC1509704), the Natural Science Foundation of China (Grant No. 41803033, 41903034), Central Plains Science and Technology Innovation Leader Project (Grant No. 214200510030) and the Research Foundation of North China University of Water Resources and Electric Power (No. 20171003). We thank Shengping Qian, Guangqian Hu, Yezhi He, Shengling Sun for their assistance in laboratory analysis. The authors also thank two anonymous reviewers and handling editor, Prof. Olaf Kolditz. The authors have declared that no conflict of interest exists.

References

Alderton DHM, Pearce JA, Potts PJ (1980) Rare earth element mobility during granite alteration: evidence from southwest England. Earth and Planetary Science Letters 49, 149-165.

Aiuppa A, Allard P, D'Alessandro W, Michel A, Parello F, Treuil M, Valenza M (2000) Mobility and fluxes of major, minor, and trace metals during basalt weathering and groundwater transport at Mt. Etna volcano (Sicily). Geochimica Et Cosmochimica Acta 64, 1827–1841.

Arıkan F, Ulusay R, Aydın N (2007) Characterization of weathered acidic volcanic rocks and a weathering classification based on a rating system. Bulletin of Engineering Geology and the Environment 66, 415–430.

Baker JH (1985) Rare earth and other trace element mobility accompanying albitization in a Proterozoic granite, W. Bergslagen, Sweden. Mineralogical Magazine 49, 107-115.

Baud P, Wong T, Zhu W (2014) Effects of porosity and crack density on the compressive strength of rocks. International Journal of Rock Mechanics and Mining Sciences 67, 202-211.

Browne PRL (1978) Hydrothermal Alteration in Active Geothermal Fields. Annual Review of Earth and Planetary Sciences 6, 229-250.

Brown ET (1981) Rock characterisation, testing and monitoring, ISRM suggested methods. International Society for Rock Mechanics. Pergamon, Oxford.

Ceryan S, Tudes S, Ceryan N (2008) Influence of weathering on the engineering properties of Harsit granitic rocks (NE Turkey). Bulletin of Engineering Geology and the Environment 67, 97–104.

Chen D (1999) Engineering geological problems in the Three Gorges Project on the Yangtze, China. Engineering Geology 51, 1–11.

Chen X, He P, Qin Z (2018) Damage to the microstructure and strength of altered granite under wet–dry cycles. Symmetry 10, 716.

Chigira M, Nakamoto M, Nakata E (2002) Weathering mechanisms and their effects on the landsliding of ignimbrite subject to vapor-phase crystallization in the Shirakawa pyroclastic f low, northern Japan. Engineering Geology 66, 111–125.

Columbu S, Gioncada A, Lezzerini M, Sitzia F (2019) Mineralogical-chemical alteration and origin of ignimbritic stones used in the old Cathedral of Nostra Signora di Castro (Sardinia, Italy). Studies in Conservation 64, 397-422.

Columbu S, Palomba M, Sitzia F, Carcangiu G (2020) Pyroclastic Stones as Building Materials in Medieval Romanesque Architecture of Sardinia (Italy): Chemical-Physical Features of Rocks and Associated Alterations. International Journal of Architectural Heritage, DOI: 10.1080/15583058.2020.1749729.

Dawood YH, Saleh GM, Abd El-Naby HH (2005) Effects of hydrothermal alteration on geochemical characteristics of the El Sukkari granite, central Eastern Desert, Egypt. International Geology Review 47, 1316-1329.

Del Potro R, Hürlimann M (2009) The decrease in the shear strength of volcanic materials with argillic hydrothermal alteration, insights from the summit region of Teide stratovolcano, Tenerife. Engineering Geology 104, 135–143.

Duzgoren-Aydin NS, Aydin A, Malpas J (2002) Re-assessment of chemical weathering indices: case study on pyroclastic rocks of Hong Kong, Engineering Geology 63, 99-119.

Farmer GL, DePaolo DJ (1987) Nd and Sr isotope study of hydrothermally altered granite at San Manuel, Arizona; implications for element migration paths during the formation of porphyry copper ore deposits. Economic Geology 82, 1142-1151.

Fritz SJ, Mohr DW (1984) Chemical alteration in the micro weathering environment within a spheroidally-weathered anorthosite boulder. Geochimica Et Cosmochimica Acta 48, 2527-2535.

Frolova YV, Ladygin VM, Rychagov SN (2012) Patterns in the transformation of the composition and properties of volcanogenic rocks in hydrothermal-magmatic systems of the Kuril-Kamchatka island arc. Moscow University Geology Bulletin 66, 430–438.

Guan P, Ng CWW, Sun M, Tang W (2001) Weathering indices for rhyolitic tuff and granite in Hong Kong. Engineering Geology 59, 147–159.

Heap M J, Xu T, Chen C (2014) The influence of porosity and vesicle size on the brittle strength of volcanic rocks and magma. Bulletin of Volcanology 76, 1-15.

Helgeson HC (1970) Description and interpretation of phase relations in geochemical processes involving aqueous solutions. American Journal of Science 268, 415-438.

Hemley JJ, Jones WR (1964) Chemical aspects of hydrothermal alteration with emphasis on hydrogen metasomatism. Economic Geology 59, 538-569.

Huang JH (2017) Alteration mineral geochemistry of VMS deposit- case study of the Honghai Cu-Zn deposit, Eastern Tianshan, NW China. Dissertation, University of Chinese Academy of Sciences. (in Chinese with English abstract)

Huang ZQ, Wang Z, Hou HM (2011) Alteration and engineering characteristics of altered-rock in Tianchi Pumped-storage power station. Journal of North China Institute of Water Conservancy and Hydroelectric Power 32, 1–5. (in Chinese with English abstract).

Hurwitz S, Ingebritsen SE, Sorey ML (2002) Episodic thermal perturbations associated with groundwater flow: An example from Kilauea Volcano, Hawaii. Journal of Geophysical Research 107, 1301-1310.

Julia F, Vladimir L, Sergey R, David Z (2014) Effects of hydrothermal alterations on physical and mechanical properties of rocks in the Kuril–Kamchatka island arc. Engineering Geology 183, 1–16.

Kahraman S, Gunaydin O, Fener M (2005) The effect of porosity on the relation between uniaxial compressive strength and point load index. International Journal of Rock Mechanics and Mining Sciences 42, 584–589.

Lan HX, Hu RL, Yue ZQ, Lee CF, Wang SJ (2003) Engineering and geological characteristics of granite weathering profiles in South China. journal of Asian Earth Sciences 21, 353–364.

Li L, Aubertin M (2003) A general relationship between porosity and uniaxial strength of engineering materials. Canadian Journal of Civil Engineering 30, 644-658.

Li XH, Li ZX, Wingate MTD, Chung SL, Liu Y, Lin GC, Li WX (2006) Geochemistry of the 755Ma Mundine Well dyke swarm, northwestern

Australia: Part of a Neoproterozoic mantle superplume beneath Rodinia? Precambrian Research 146, 1–15.

Lv CX, Wu GG, Chen XL, Zhang YC, Zhang XY, Zhao, H (2011) Structural and geochemical characteristics of alteration zone of Xincheng gold deposit. Geotectonica et Metallogenia 35, 618-627. (in Chinese with English abstract)

Ma TF (2014) Research on High strength concrete strength survey based on rebound method in Hebei. Dissertation, Hebei University of Technology. (in Chinese with English abstract).

Ma L, Chen Q, Zhu J, Xi Y, He H, Zhu R, Ayoko GA (2016) Adsorption of phenol and Cu (II) onto cationic and zwitterionic surfactant modified montmorillonite in single and binary systems. Chemical Engineering Journal 283, 880-888.

Meller C, Kontny A, Kohl T (2014) Identification and characterization of hydrothermally altered zones in granite by combining synthetic clay content logs with magnetic mineralogical investigations of drilled rock cuttings. Geophysical Journal International 199, 465-479.

Miao C (2017) Study on influence of altered-rock to geological characteristics and its engineering—exemplified by Dagangshan Hydropower station. Dissertation, Chengdu University of Technology.

Moon V, Jayawardane J (2004) Geomechanical and geochemical changes during early stages of weathering of Karamu Basalt, New Zealand. Engineering Geology 74, 57–72.

Palchik V, Hatzor YH (2004) The influence of porosity on tensile and compressive strength of porous chalks. Rock Mechanics and Rock Engineering 37, 331-341.

Parry WT, Downey LM (1982) Geochemistry of hydrothermal chlorite replacing igneous biotite. Clays and Clay Minerals 30, 81-90.

Pola A, Crosta G, Fusi N, Barberini V, Norini G (2012) Influence of alteration on physical properties of volcanic rocks. Tectonophysics 566-567, 67–86.

Pola A, Crosta GB, Fusi N, Castellanza R (2014) General characterization of the mechanical behaviour of different volcanic rocks with respect to alteration. Engineering Geology 169, 1–13.

Qin Z, Fu H, Chen X (2019) A study on altered granite meso-damage mechanisms due to water invasion-water loss cycles. Environmental Earth Sciences 78, 1-10.

Saar M O, Manga M (1999) Permeability-porosity relationship in vesicular basalts. Geophysical Research Letters 26, 111-114.

Sharma A, Rajamani V (2000) Major Element, REE, and Other Trace Element Behavior in Amphibolite Weathering under Semiarid Conditions in Southern India. The Journal of Geology 108, 487–496.

Shea T, Houghton BF, Gurioli L, Cashman KV, Hammer JE, Hobden BJ (2010) Textural studies of vesicles in volcanic rocks: an integrated methodology. Journal of Volcanology and Geothermal Research 190, 271-289.

Sumner P, Nel W (2002) The effect of rock moisture on Schmidt hammer rebound: tests on rock samples from Marion Island and South Africa. Earth Surf. Process. Landforms 27, 1137–1142.

Sun, SS, McDonough WF (1989) Chemical and isotopic systematics of oceanic basalts: Implications for mantle composition and processes. Geological Society, London, Special Publications 42, 313–345.

Ulusay R, Türeli K, Ider MH (1994) Prediction of engineering properties of a selected litharenite sandstone from its petrographic characteristics using correlation and multivariate statistical techniques. Engineering Geology 38, 135-157.

Ündül Ö (2016) Assessment of mineralogical and petrographic factors affecting petro-physical properties, strength and cracking processes of volcanic rocks. Engineering Geology 210, 10-22.

Wang AM, Li XG, Huang ZQ, Huang XC, Wang ZF, Wu Q, Cui JL, Lu XJ (2015) Laboratory study on engineering geological characteristics and formation mechanism of altered rocks of Henan Tianchi pumped storage power station, China. Environmental Earth Sciences 74, 5063–5075.

Wang AM, Zhou J, Zhong FW, Wu Q, Cui JL (2013) Characteristics Analysis of Rock Weathering and Alteration for Tianchi Pumped Storage Power Station.

Journal of North China Institute of Water Conservancy and Hydroelectric Power 8, 21–25. (in Chinese with English abstract)

Watters (2000) Rock Mass Strength Assessment and Significance to Edifice Stability, Mount Rainier and Mount Hood, Cascade Range Volcanoes. Pure and applied geophysics 157, 957–976.

Wyering LD, Villeneuve MC, Wallis IC, Siratovich PA, Kennedy BM, Gravley DM, Cant JL (2014) Mechanical and physical properties of hydrothermally altered rocks, Taupo Volcanic Zone, New Zealand. Journal of Volcanology and Geothermal Research 288, 76–93.

Xu DR, Wang L, Li PC, Chen GH, He ZL, Fu GG, Wu J (2009) Petrogenesis of Lianyunshan granites in northeastern Hunan Province, South China, and its geodynamic implications. Acta Petrologica Sinica 25, 1–23. (in Chinese with English abstract)

Xu R, Romer RL, Glodny J (2020) External fluids cause alteration and metal redistribution in the granite-hosted Tangziwa SnCu deposit, Gejiu district, China. Lithos, https://doi.org/10.1016/j.lithos.2020.105937.

Yang GL (2007) Altered-rock characteristics and its engineering respondences studying—exemplified by Xiaowan hydropower station, Lancang revier. Dissertation, Chengdu University of Technology.

Yıldız A, Kuşcu M, Dumlupunar I, Arıtan AE, Bağcı M (2010) The determination of the mineralogical alteration index and the investigation of the efficiency of the hydrothermal alteration on physico-mechanical properties in volcanic rocks from Köprülü, Afyonkarahisar, West Turkey. Bulletin of engineering geology and the environment 69, 51-61.

Zhang W (1991) Structural and geochemical features of the Changsha-Pingjiang fracture dynamic metamorphism zone in NE. Hunan Province, China. Geotectonica et Metallogenia, 100–109. (in Chinese with English abstract)

Table 1. Physical parameters and mineral compositions of the granite samples in Pingjiang

Samples	Altered type	Physical parameters			Mineral composionts							
		Dry bulk density (g/cm3)	Particle density (g/cm3)	Porosity (%)	Quartz (%)	Orthoclase (%)	Plagioclase (%)	Biotite (%)	Chlorite (%)	Kaolinite (%)	Smectite (%)	Illite (%)
SPD3-2	WA	2.32	2.59	10.42	20-25	20-25	30-35			5	10-15	5-10
XP4-1	WA	2.19	2.58	15.12	25-30		25-30	15-20	5-10	5-10	5-10	5
XP4-2	WA				20-25	2	2			25-30	25-30	5-10
SPD2-4	HA	2.41	2.62	8.02	20-30	20-25	25-30	10-15	3-5	5-10		
SPD2-5	HA	2.58	2.65	2.64	25-30	15-20	30-35	5-10	3-5	3-5		
PD2-4	SZ				60-75	10-15	5-10	5-10	5	3-5		
PD2-7	F	2.65	2.67	0.75	25-30	15-20	35-40	5-10	3-5	2		

Table 2. Results of geochemical analysis and mechanical tests for granite samples in Pingjiang

Sample	PD 2-1	PD 2-2	PD 2-4	PD 2-5	PD 2-6	PD 2-7	PD 2-8	SPD 2-5	PD 2-9	PD 2-10	PD 2-11	SPD 2-4	SPD 2-3	XP 4-200		SPD 3-2	SPD 3-3	SPD 3-4	XP 4-1	XP 4-2	XP 4-3
	Silicified fracture zone (SZ)					Fresh	Hydrothermally altered (HA)									Weathered (WA)					
Major oxides (%)																					
Na_2O	3.74	3.84	1.87	3.53	3.15	3.70	3.97	3.50	3.89	4.11	4.14	3.41	3.17	2.76		2.46	3.81	2.52	2.16	0.32	1.87
MgO	0.31	0.47	0.23	0.47	0.45	0.65	0.56	0.68	0.53	0.50	0.48	0.71	0.65	0.40		0.80	0.91	0.85	1.58	2.55	0.60
Al_2O_3	12.0	12.3	7.20	12.1	12.7	15.4	15.0	14.9	15.5	15.2	16.1	14.9	15.3	14.8		17.6	14.8	17.6	18.6	19.2	16.6
SiO_2	77.4	75.9	85.6	76.7	76.3	70.7	72.0	72.1	71.1	71.2	70.7	71.8	71.8	72.7		68.4	71.0	68.2	64.0	56.6	70.9
K_2O	2.80	3.24	1.57	2.87	2.97	3.58	3.43	3.31	4.11	4.15	2.83	3.29	3.20	4.95		2.96	2.39	2.75	1.57	1.63	3.22
CaO	1.41	1.01	1.34	1.00	1.40	2.59	1.50	2.64	0.72	0.38	2.55	2.64	2.50	1.47		1.80	2.97	1.80	2.29	0.67	0.83
TiO_2	0.18	0.23	0.11	0.23	0.22	0.27	0.24	0.21	0.27	0.25	0.23	0.23	0.22	0.12		0.27	0.28	0.28	0.45	1.07	0.19
Fe_2O_{3T}	1.27	1.72	0.88	1.73	1.49	1.92	1.63	1.74	1.87	1.83	1.68	2.01	1.82	1.26		2.43	2.51	2.53	4.48	9.90	2.13
LOI	0.69	0.85	0.53	1.18	1.09	0.74	1.02	0.97	1.41	1.58	0.84	1.01	1.35	1.52		3.29	1.35	3.50	4.87	8.14	3.68
Trace elements (ppm)																					
Ba	740	77.1	-	949	946	1062	1108	-	836	889	816	-	-	-	-	-	-	-	-	-	-
Th	9.57	3.93	-	14.3	12.5	14.7	15.0	-	13.6	13.0	12.3	-	-	-	-	-	-	-	-	-	-
Nb	4.61	3.87	-	5.91	5.59	5.66	4.94	-	4.70	4.28	5.19	-	-	-	-	-	-	-	-	-	-
La	16.1	16.3	-	12.4	23.1	41.1	38.8	-	28.1	32.9	24.2	-	-	-	-	-	-	-	-	-	-
Ce	30.8	35.6	-	23.3	42.8	74.7	70.6	-	56.3	63.6	48.0	-	-	-	-	-	-	-	-	-	-
Pb	14.1	6.29	-	33.8	36.1	43.2	46.0	-	43.7	38.2	40.5	-	-	-	-	-	-	-	-	-	-
Rb	133	5.99	-	178	213	172	172	-	182	202	130	-	-	-	-	-	-	-	-	-	-
Sr	315	71.5	-	303	451	605	603	-	301	194	459	-	-	-	-	-	-	-	-	-	-
Zr	92.4	124	-	138	128	156	148	-	128	121	117	-	-	-	-	-	-	-	-	-	-
Hf	2.75	3.44	-	3.93	3.55	4.48	4.17	-	3.96	3.71	3.67	-	-	-	-	-	-	-	-	-	-
Sm	1.79	4.41	-	1.47	2.43	4.18	4.00	-	3.35	3.48	2.71	-	-	-	-	-	-	-	-	-	-
Eu	0.49	1.15	-	0.52	0.66	0.94	0.86	-	0.79	0.77	0.74	-	-	-	-	-	-	-	-	-	-
Ti	883	2687	-	1189	1170	1584	1296	-	1241	1174	1016	-	-	-	-	-	-	-	-	-	-
Gd	1.40	4.51	-	1.48	1.87	2.98	2.82	-	2.54	2.55	2.11	-	-	-	-	-	-	-	-	-	-
Tb	0.16	0.74	-	0.17	0.21	0.32	0.30	-	0.27	0.26	0.23	-	-	-	-	-	-	-	-	-	-
Dy	0.79	4.75	-	0.85	1.02	1.40	1.35	-	1.24	1.19	1.09	-	-	-	-	-	-	-	-	-	-
Y	3.97	29.4	-	4.72	5.27	6.46	6.23	-	5.13	4.78	4.45	-	-	-	-	-	-	-	-	-	-
Ho	0.14	1.07	-	0.16	0.18	0.23	0.22	-	0.21	0.20	0.19	-	-	-	-	-	-	-	-	-	-
Er	0.37	3.35	-	0.45	0.45	0.57	0.58	-	0.53	0.50	0.46	-	-	-	-	-	-	-	-	-	-
Tm	0.05	0.51	-	0.07	0.06	0.08	0.08	-	0.08	0.07	0.07	-	-	-	-	-	-	-	-	-	-
Yb	0.34	3.53	-	0.43	0.43	0.52	0.51	-	0.47	0.44	0.43	-	-	-	-	-	-	-	-	-	-
Lu	0.05	0.59	-	0.06	0.06	0.08	0.08	-	0.07	0.06	0.07	-	-	-	-	-	-	-	-	-	-
Mechanical tests																					
V_p (Km/s)	2.00	1.10	4.04	4.88	5.11	4.33	4.23	4.21	4.50	3.92	4.86	3.69	1.49	6.11		0.51	0.55	0.63	0.35	0.51	0.40
$I_{s(50)}$ (Kpa)	4468	5382	5053	4069	1036	4991	4310	5946	2930	364	2948	838	50.0	76273		4.69	5.04	8.91	4.70	4.90	4.80
Rebound	28	32	28	29	25	30	32	56	30	25	31	24	22	69		11	20	24	12	14	12

Figure captions:

Fig. 1. Geological map of Pingjiang (modified from Xu et al., 2009).

Fig. 2. Geological map of Fushou mountain and geological sketch of the PD2 adit (modified from Xu et al., 2009).

Fig. 3. Photomicrographs of thin section and photographs of silicified fracture zone. (a) Biotite and orthoclase were partly altered to chlorite and albite, respectively. (b) Cataclastic texture and feldspars were altered to argillic minerals. (c) Granite is broken into breccia and quartz refilled at the end of PD2. (d) Granite is replaced by quartz. Abbreviations: Ab=albite, Bt=biotite, Chl=chlorite, Or=orthoclase, Pl=plagioclase, Qtz=quartz.

Fig. 4. Plots of rebound value versus point load strength index (a) and V_p (b).

Fig. 5. Plots of LOI versus V_p (a), rebound value (b) and point load strength index (c, d).

Fig. 6. Plots of LOI versus Na_2O (a), CaO (b), K_2O (c), SiO_2 (d), MgO (e) and Fe_2O_{3T} (f).

Fig. 7. Primitive mantle normalized trace element patterns (a) and Chondrite-normalized rare earth elements patterns (b) for the samples from PD2. Compositions of chondrite and primitive mantle are from Sun and McDonough (1989).

Fig. 8. MI of major elements and trace elements normalized to Al_2O_3.

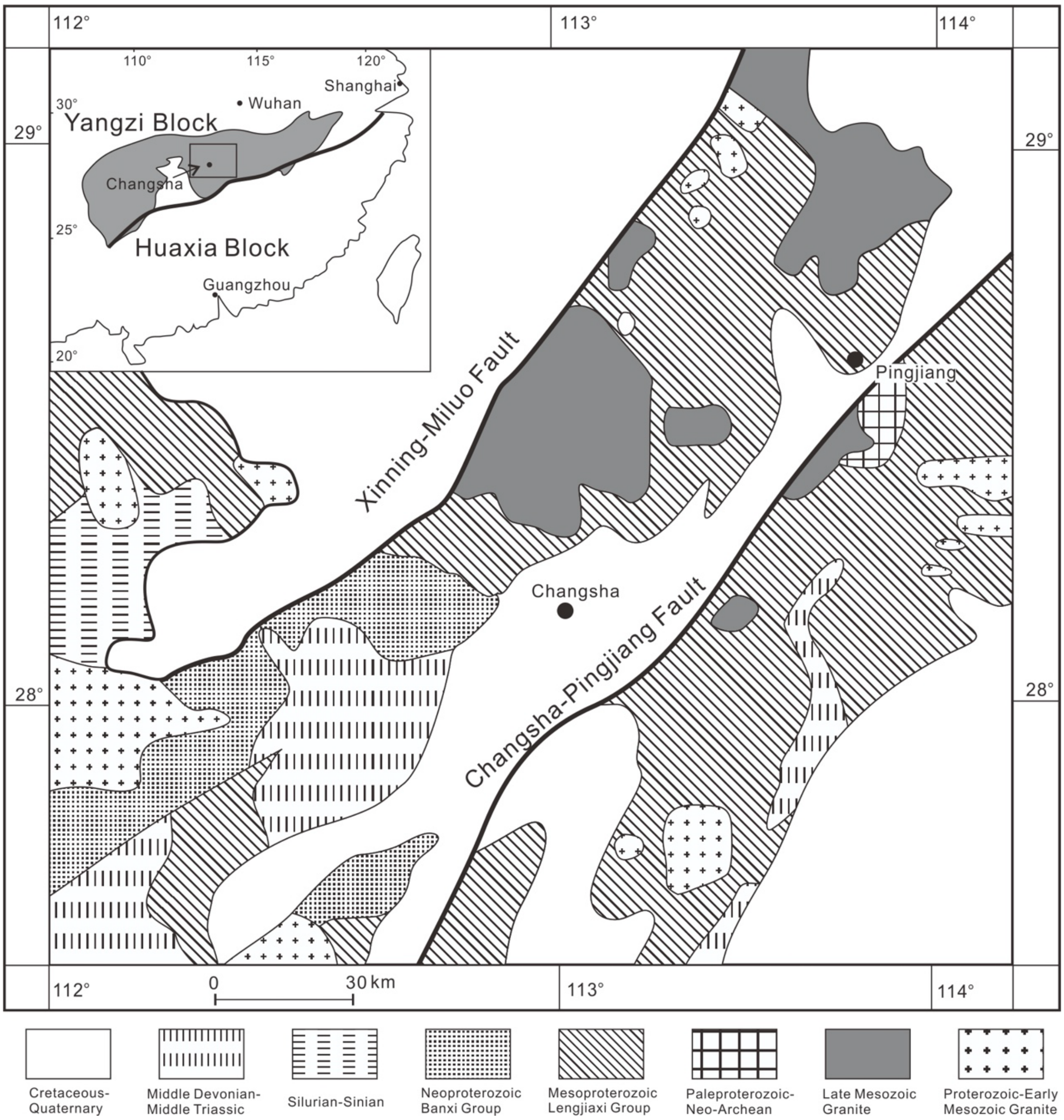

112°
113°
114°
29°
28°
110°
115°
120°
30°
25°
20°
Wuhan
Shanghai
Yangzi Block
Changsha
Huaxia Block
Guangzhou
Xinning-Miluo Fault
Pingjiang
Changsha
Changsha-Pingjiang Fault
0
30 km
Cretaceous-Quaternary
Middle Devonian-Middle Triassic
Silurian-Sinian
Neoproterozoic Banxi Group
Mesoproterozoic Lengjiaxi Group
Paleoproterozoic-Neo-Archean
Late Mesozoic Granite
Proterozoic-Early Mesozoic Granite

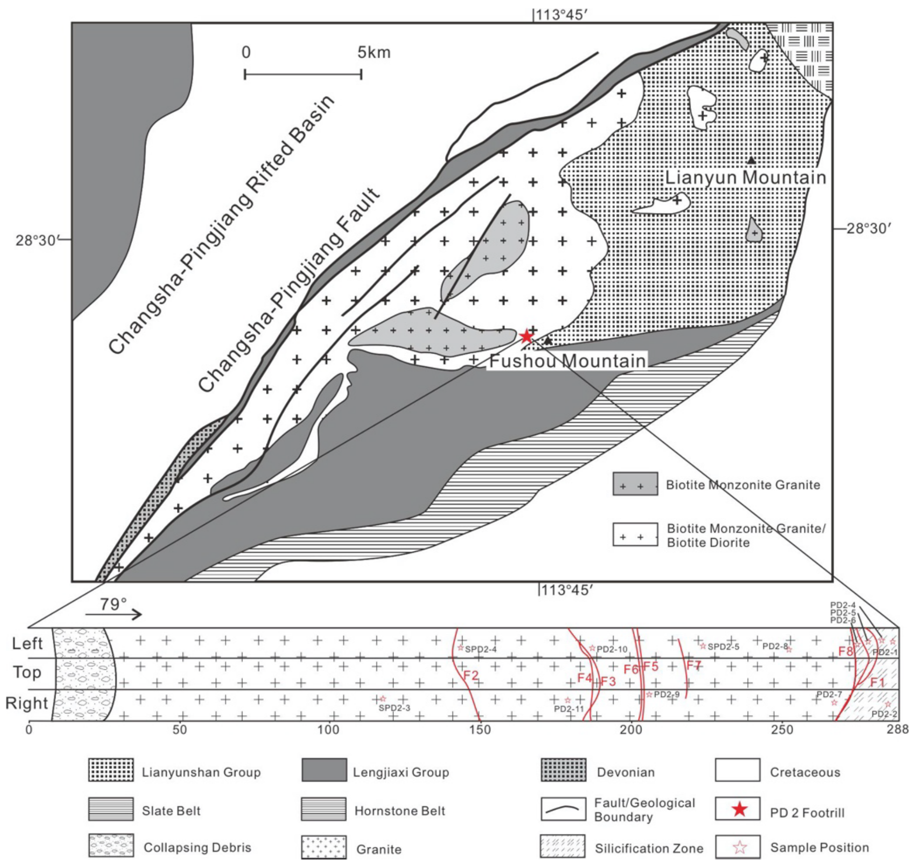

113°45′
0
5km
Changsha-Pingjiang Rifted Basin
Changsha-Pingjiang Fault
Lianyun Mountain
Fushou Mountain
28°30′
28°30′
Biotite Monzonite Granite
Biotite Monzonite Granite/
Biotite Diorite
113°45′
79°
Left
Top
Right
SPD2-4
PD2-10
SPD2-5
PD2-8
PD2-4
PD2-5
PD2-6
PD2-1
F2
F4
F3
F6
F5
F7
F8
F1
SPD2-3
PD2-11
PD2-9
PD2-7
PD2-2
0
50
100
150
200
250
288
Lianyunshan Group
Lengjiaxi Group
Devonian
Cretaceous
Slate Belt
Hornstone Belt
Fault/Geological Boundary
PD 2 Footrill
Collapsing Debris
Granite
Silicification Zone
Sample Position

Fig. 2.

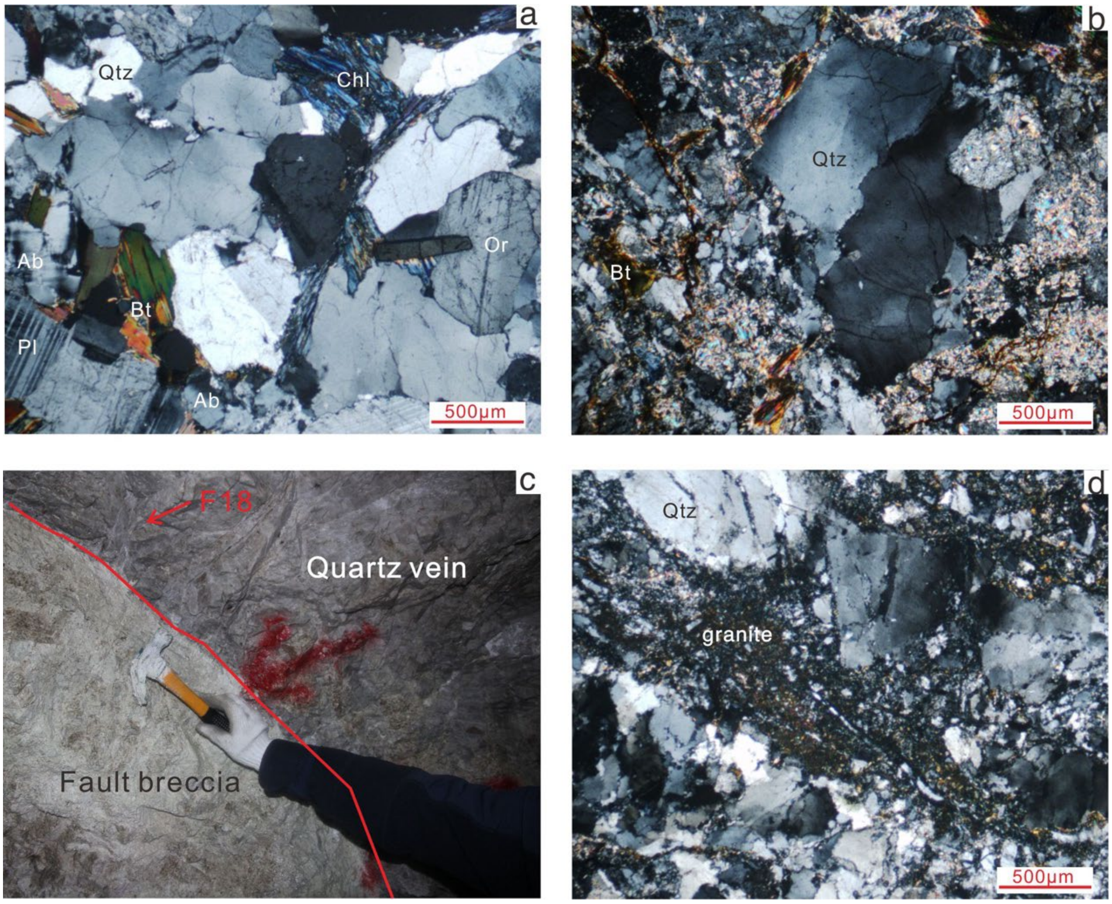
a
Qtz
Chl
Or
Ab
Bt
Pl
Ab
500μm
b
Qtz
Bt
500μm
c
F18
Quartz vein
Fault breccia
d
Qtz
granite
500μm

Fig. 3.

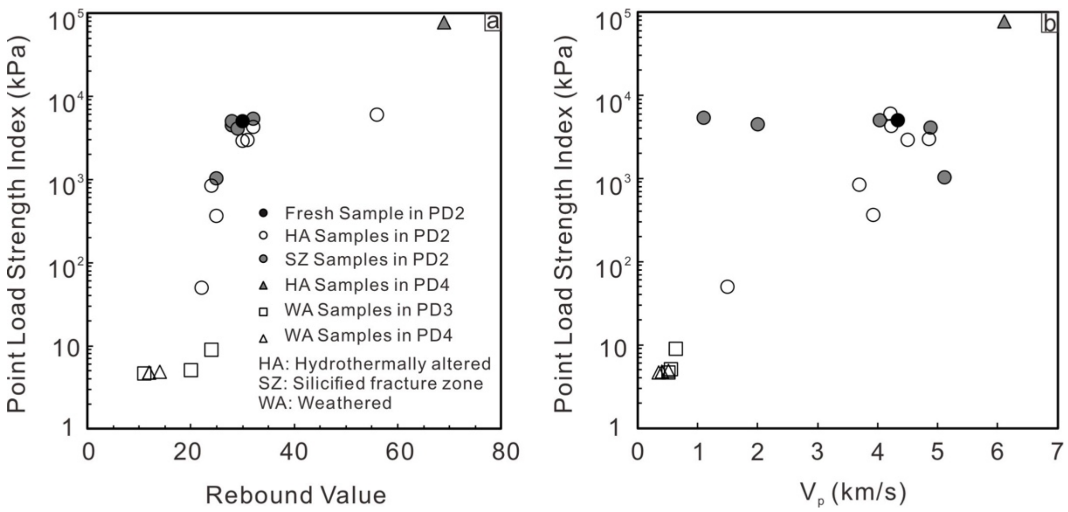
Point Load Strength Index (kPa)
Rebound Value
a
Fresh Sample in PD2
HA Samples in PD2
SZ Samples in PD2
HA Samples in PD4
WA Samples in PD3
WA Samples in PD4
HA: Hydrothermally altered
SZ: Silicified fracture zone
WA: Weathered
Point Load Strength Index (kPa)
V$_p$ (km/s)
b

Fig. 4.

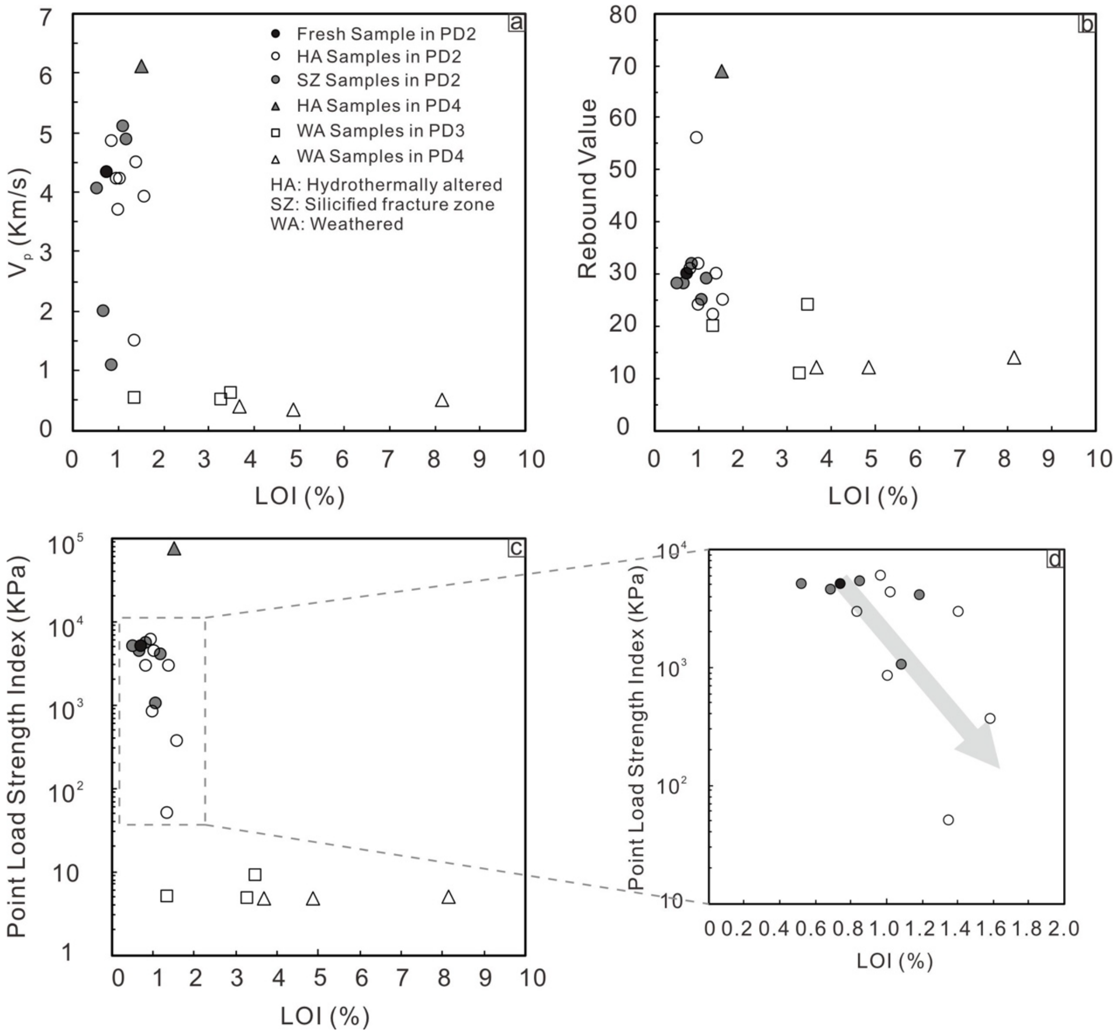
a
Fresh Sample in PD2
HA Samples in PD2
SZ Samples in PD2
HA Samples in PD4
WA Samples in PD3
WA Samples in PD4
HA: Hydrothermally altered
SZ: Silicified fracture zone
WA: Weathered
Vp (Km/s)
LOI (%)
b
Rebound Value
LOI (%)
c
Point Load Strength Index (KPa)
LOI (%)
d
Point Load Strength Index (KPa)
LOI (%)

Fig. 5.

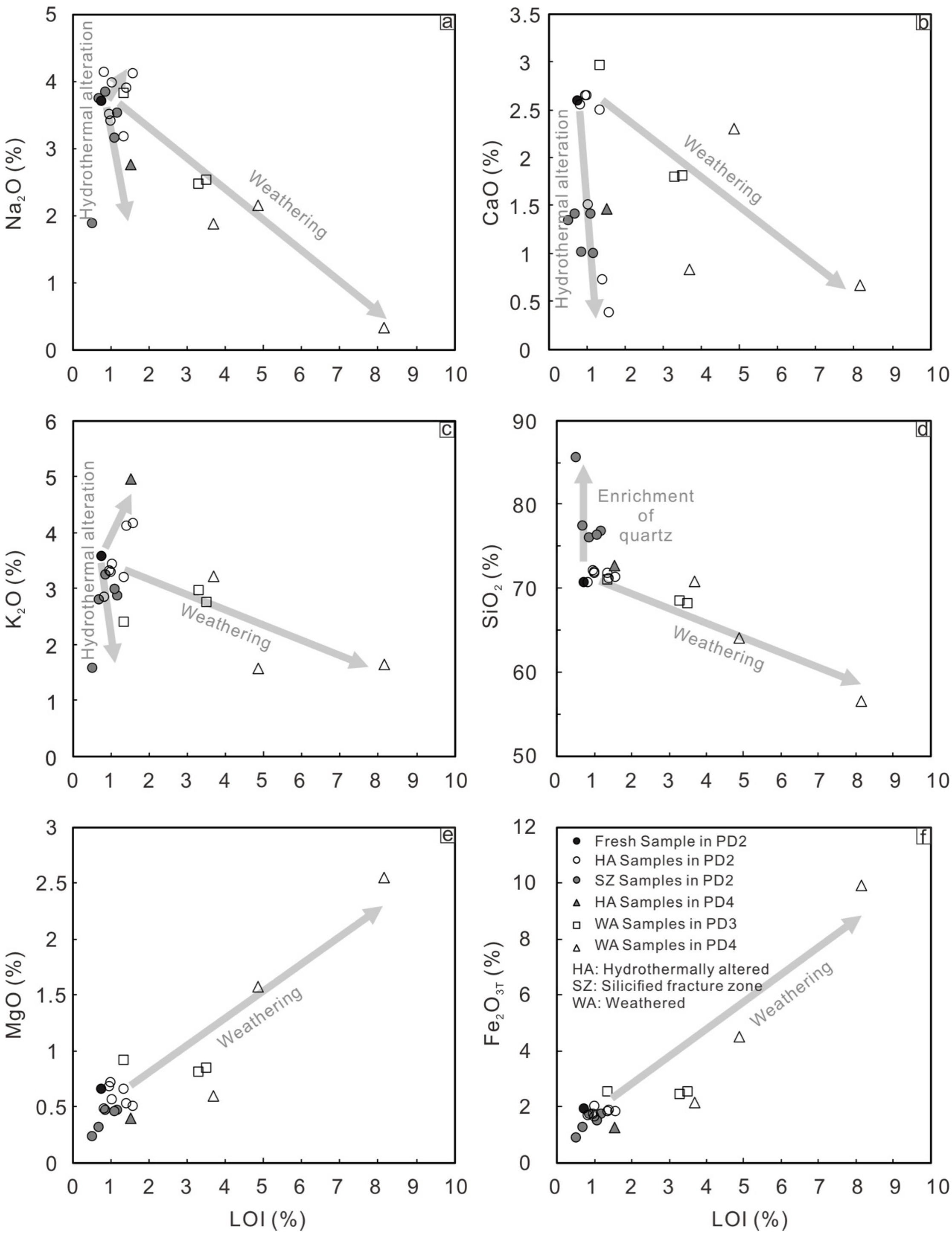

a
b
c
d
e
f
Na2O (%)
CaO (%)
K2O (%)
SiO2 (%)
MgO (%)
Fe2O3T (%)
LOI (%)
Hydrothermal alteration
Weathering
Enrichment of quartz
Fresh Sample in PD2
HA Samples in PD2
SZ Samples in PD2
HA Samples in PD4
WA Samples in PD3
WA Samples in PD4
HA: Hydrothermally altered
SZ: Silicified fracture zone
WA: Weathered

Fig. 6.

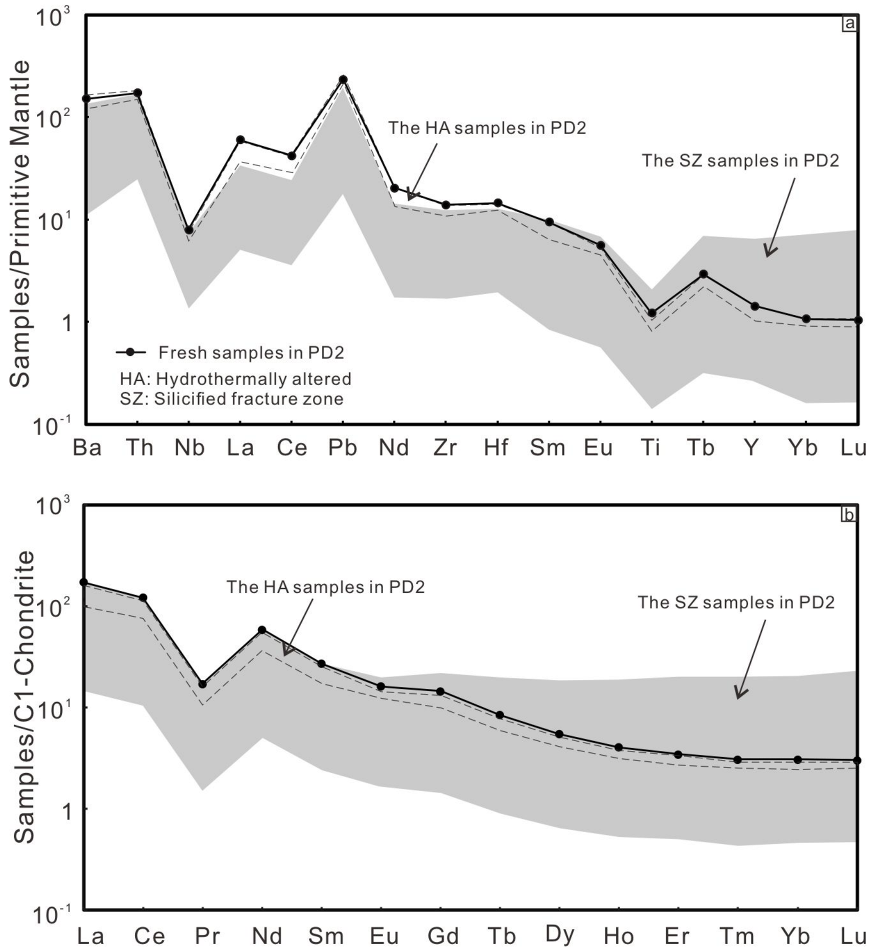

a
Samples/Primitive Mantle
10³
10²
10¹
1
10⁻¹
Ba
Th
Nb
La
Ce
Pb
Nd
Zr
Hf
Sm
Eu
Ti
Tb
Y
Yb
Lu
The HA samples in PD2
The SZ samples in PD2
Fresh samples in PD2
HA: Hydrothermally altered
SZ: Silicified fracture zone
b
Samples/C1-Chondrite
The HA samples in PD2
The SZ samples in PD2
La
Ce
Pr
Nd
Sm
Eu
Gd
Tb
Dy
Ho
Er
Tm
Yb
Lu

Fig. 7.

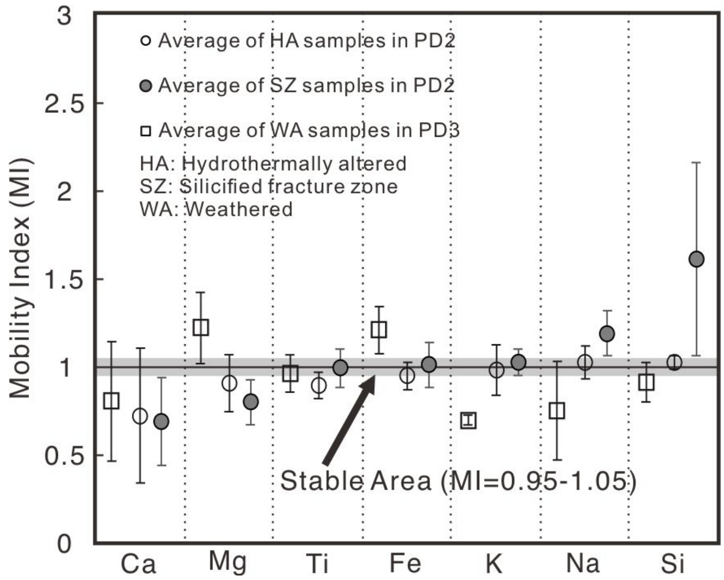
Average of HA samples in PD2
Average of SZ samples in PD2
Average of WA samples in PD3
HA: Hydrothermally altered
SZ: Silicified fracture zone
WA: Weathered
Mobility Index (MI)
Stable Area (MI=0.95-1.05)
Ca
Mg
Ti
Fe
K
Na
Si
3
2.5
2
1.5
1
0.5
0

Fig. 8.